



Photoinitiation rate profiles during polymerization of a dimethacrylate-based resin photoinitiated with camphorquinone/amine. Influence of initiator photobleaching rate

Silvana Asmussen^a, Gustavo Arenas^b, Wayne D. Cook^c, Claudia Vallo^{a,*}

^aInstituto de Investigación en Ciencia y Tecnología de Materiales, Mar del Plata University -National Research Council (CONICET), Av. Juan B. Justo 4302, 7600 Mar del Plata, Argentina

^bDepartment of Physics, Engineering School, Mar del Plata University, Argentina

^cDepartment of Materials Engineering, Monash University, Melbourne, Victoria, Australia

ARTICLE INFO

Article history:

Received 29 August 2008

Received in revised form 28 October 2008

Accepted 5 November 2008

Available online 12 November 2008

Keywords:

Photopolymerization

Photobleaching

Camphorquinone

Dimethacrylates

ABSTRACT

The photodecomposition of camphorquinone (CQ)/amine during the photo polymerization of a dimethacrylate-based resin under continuous irradiation was investigated in thick samples. The global CQ photoconsumption was measured by monitoring the decrease in light absorption as a function of irradiation time and the kinetics were satisfactory fitted to a first order expression where the rate constant of photobleaching was proportional to the irradiation intensity. In a thick sample, the photobleaching of the photoinitiator is accompanied by a deeper penetration of the light through the underlying layers. These gradients of photoinitiator concentration, light intensity and photoinitiation rate along the path of irradiation were calculated. The photodecomposition reaction was spatially inhomogeneous and the degree of nonuniformity increased with increased initial sample absorbance. The influence of the photobleaching process on the polymerization reaction was examined. The photobleaching rate of CQ was much slower than the polymerization rate and only 20% of the initial amount of CQ was consumed before the polymerization reaction had almost ceased. Results obtained in this research highlight the inherent interlinking of light attenuation and photobleaching rate in bulk polymerizing systems.

© 2008 Elsevier Ltd. All rights reserved.

1. Introduction

Dimethacrylate monomers are commonly used as the organic matrix of dental restorative composites materials. The rapid network formation of monomer mixtures such as bisphenol-A diglycidyl ether dimethacrylate (bis-GMA) and triethylene glycol dimethacrylate (TEGDMA) is beneficial in clinical applications since highly crosslinked polymers are produced at relatively short cure times. Polymerization of dental resins is generally initiated by the camphorquinone (CQ)/amine photo-initiating system, which produces free radicals on exposure to 450–500 nm

radiation [1,2]. Photopolymerization at high initiator concentration is attractive in dental applications because spatially averaged polymerization rates typically increase as initiator concentration increases. However, many studies have shown that polymerization rate reaches a maximum for an optimum level of photoinitiator, and then decreases due to radiation attenuation in the underlying layers [1,3–5].

The effect of the attenuation of the light intensity along the radiation path is a well known factor in photo-processes that take place in bulk as well as in films [6–12]. In a photo-reactive initiator system, there is a spatio-temporal distribution of both light intensity and photoinitiator concentration. Initially, the initiator concentration is uniform, and the light intensity will decrease with depth

* Corresponding author. Fax: +54 223 4816600.
E-mail address: civallo@fi.mdp.edu.ar (C. Vallo).

according to the Beer–Lambert law. Immediately after irradiation, the initiator will be consumed at a rate proportional to the local light intensity, thereby leading to an initiator concentration gradient along the beam direction. This leads to temporal variation of local light intensity – depending on the nature of the photolysis products, this consumption of the photoinitiator can either lead to an increase in light intensity in the underlying layers (if the photolysis product is more transparent at the irradiating wavelengths) or, in some cases, a reduction in light intensity (if the photolysis product is strongly absorbing or in light scattering media [13–16]). Thus, a mathematical description of photoinitiation process with a photobleaching photoinitiator must take into account the coupling of the effect of light intensity gradient and the initiator concentration gradient. In a recent report, Terrones et al. [8,9] discussed the inherent inability of the standard theoretical treatments of photopolymerization kinetics to account for the spatial variation of the initiation rate with photobleaching initiators.

The attenuation of the radiation as a function of depth into the material not only affects the cure kinetics but also often limits the depth of cure. Experimentally, the contribution of attenuation to spatial variation in photopolymerization kinetics has been identified in dental applications. Since light activated dental composites are normally used in thick section, the depth of cure is important due to its affect on the properties of undercured material and the presence of potentially toxic residual monomer which can be eluted from the resin into the tissues. The photolysis of photoinitiators in organic solvents has been widely studied during the last two decades, however, studies of the photobleaching of photoinitiators in polymerizing monomers have not received the same attention. Thus, the purpose of this work, was to study the photodecomposition of CQ during photopolymerization of a dimethacrylate-based dental resin, and to analyze the influence of the photobleaching rate on the spatiotemporal distribution of photoinitiation rates. Results of local photoinitiator concentration, light intensity and photoinitiation rate in systems with different initial absorbance are presented. The influence of the photo-decomposition rate of CQ on photoinitiation rates profiles was investigated for light emitting diode (LED) sources of relatively low intensity as well as for commercial dental photocuring sources of high intensity.

2. Experimental section

2.1. Materials

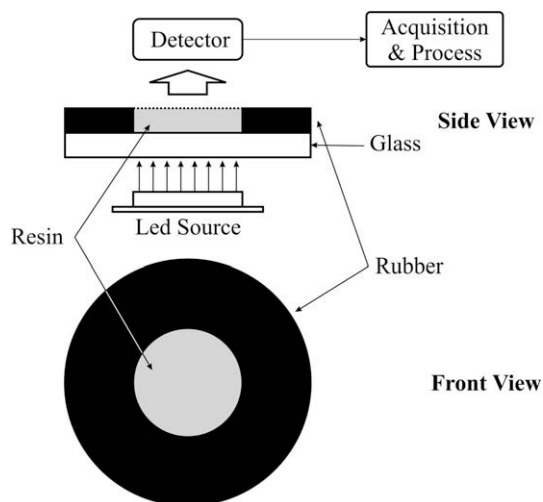
The resin formulation used for this study was 70:30 weight ratio of 2,2-bis[4-(2-hydroxy-3-methacryloxyprop-1-oxy)phenyl]propane (commonly known as bisphenol-A diglycidyl ether dimethacrylate or bis-GMA) and triethylene glycol dimethacrylate (TEGDMA). bis-GMA (Esstech, Essington, PA) and TEGDMA (Aldrich) were used as received. The resins were activated for visible light polymerization by the addition of 1 wt% CQ (Aldrich) in combination with an equimolar amount (0.90 wt%) of dimethylamino ethylmethacrylate (DMAEMA, Aldrich).

2.2. Light sources

The light source employed was assembled from a LED with its emittance centred at 470 nm (LED, OTLH-0090-BU, Optotech, Inc.). The LED was selected in order to obtain an optimum overlap between the spectral irradiance of the curing unit and the absorption spectrum of CQ. The relative emission spectrum of the LED source was measured with a calibrated CVI-monochromator (Digikrom 480) and was found to lie within the range 430–520 nm. The diameter of the irradiation area was 10 mm, which is equal to photocuring sample's diameter. The intensity of the LED was set at three different values by varying the electrical voltage through the semiconductor: 30, 75 and 140 mW. The absolute, total intensity of the LED was measured with the chemical actinometer, potassium ferrioxalate, which is recommended for the 253–577 nm wavelength range.

2.3. Photobleaching of CQ

The DMAEMA amine and bis-GMA/TEGDMA resins do not absorb significantly between 420 and 520 nm so that the photobleaching of the CQ can be assessed by monitoring the decrease in light absorption as a function of continuous irradiation time. The absorption changes were studied by recording the transmitted light that passed through samples of bis-GMA/TEGDMA containing CQ/DMAEMA. The resin was contained in a 10 mm diameter well constructed from a rubber gasket material and with a glass slide (Scheme 1). The light intensity that passed through the perforation in the rubber gasket, was measured by the actinometer and the resulting irradiances were 5.0, 12.8 and 21.6 mW/cm². The thickness of the samples was varied in the range 1–2 mm. The photodetector of the transmitted light was an OPHIR device (OPHIR Optronics, Israel), PD 2000, range 2 μW–200 mW, precision ±3%. The light source was placed underneath the sample and in contact with the glass substrate. The detector (with a 10 mm diameter sensing area) was placed above and at



Scheme 1. Experimental setup for transmitted light measurement.

the centre of the sample at a distance <1 mm in order to collect and measure all of the transmitted light as a function of irradiation time. Measurements were also carried out in resins without photoinitiator to correct for the radiation scattered/reflected at the air/glass/resin/air interfaces. Three replicates of each test were performed.

3. Results and discussion

Measurements of transmitted light were carried out during photopolymerization of the resin. The reaction is highly exothermic, and consequently, the temperature of the resin increases during the measurement [17–18]. In a previous study [17], we reported the simultaneous conversion of double bonds, heat generation and shrinkage using the same experimental setup as that described above. Thus, the present study of the photobleaching of CQ facilitates the comparison of photopolymerization and photodecomposition rate measurements with temperature rise and shrinkage. CQ absorbs in the 450–500 nm region of the visible light spectrum and so displays an intense dark yellow colour due to the presence of two carbonyl chromophores. During irradiation, the CQ decomposes into colorless products. Fig. 1 is a typical plot of the recorded transmitted light and the absorbed light (corrected by subtraction of the light lost by scattering at the sample interfaces or absorbed by the resin alone) by the CQ as a function of irradiation time. The decomposition rate constant was calculated taking into account that the rate of photodecomposition of CQ is proportional to the volumetric rate of absorption of photons. The number of photons absorbed per unit time through a sample thickness L is given by

$$I_{abs} = I_0(1 - e^{-\varepsilon CQL}) \quad (1)$$

where CQ is the molar concentration of CQ averaged over the sample thickness, and ε is the wavelength dependent absorption coefficient of CQ equal to 2.302 times its extinc-

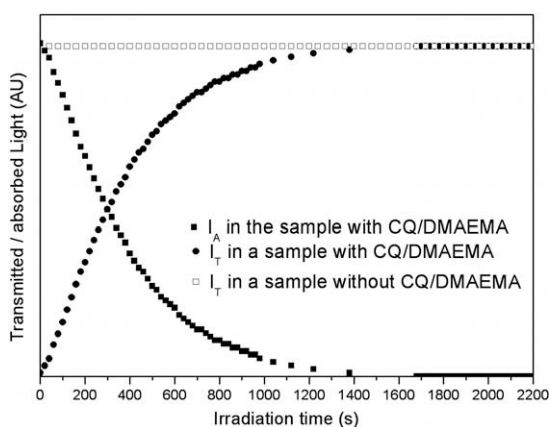


Fig. 1. Corrected transmitted and absorbed light intensity vs. irradiation time for bis-GMA/TEGDMA/CQ/DMAEMA. The irradiance was 5.0 mW/cm². The ordinate is in arbitrary units. Some points were removed in order to make the plot clearer. Also included is the measured transmitted light intensity vs. irradiation time in a resin sample without CQ/DMAEMA, indicating that the resin spectrum is not altered by the irradiation.

tion coefficient (42 ± 2 l/mol cm) [1,19]. The rate of decomposition of CQ is related to the quantum yield and the radiation absorbed [8,9]:

$$-\frac{dCQ}{dt} = \frac{\Phi I_{abs}}{L} = \frac{\Phi I_0(1 - e^{-\varepsilon LCQ})}{L} \quad (2)$$

where I_0 is the irradiance (in moles photons/s/cm²) at the base of the sample and Φ , which is usually termed the quantum yield of the photoinitiator consumption, is the fraction of photoinitiator reduced per absorbed photon. In the present case Φ is a constant that includes the rates of intersystem crossing of the excited singlet to the triplet state, formation of the exciplex state with amine and formation of radicals as well as the rate constants for the deactivation of the excited singlet and the triplet states [1]. Integrating Eq. (2) yields:

$$\ln \left[\frac{(10^{\varepsilon LCQ} - 1)}{(10^{\varepsilon LCQ_0} - 1)} \right] = \Phi \varepsilon I_0 t \quad (3)$$

where $(\Phi \varepsilon I_0)$ is the CQ rate constant for the photobleaching of CQ and CQ_0 is the initial concentration of CQ. Plots of Eq. (3) versus irradiation time measured with LEDs sources of different intensity are presented in Fig. 2. Results presented in Table 1 show that the rate constant for the photobleaching of CQ, calculated from the slope of the lines presented in Fig. 2 was proportional to the irradiance. From the value of the photobleaching rate constant $(\Phi \varepsilon I_0)$ of CQ, the volume averaged CQ concentration versus irradiation time was calculated with the following expression [8]:

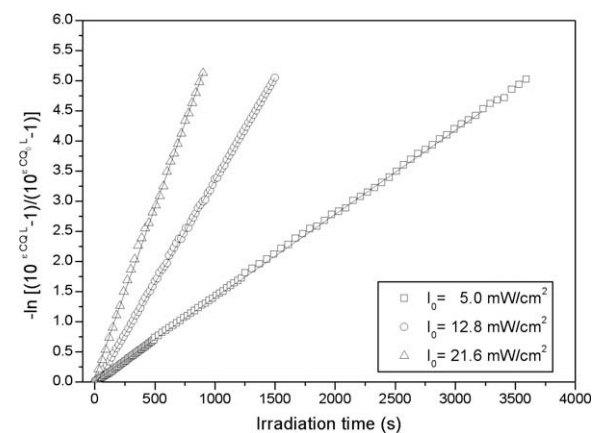


Fig. 2. Plots of Eq. (4) for different light irradiances. The regression coefficients were >0.99.

Table 1

CQ decomposition rates constant $(\Phi \varepsilon I_0)$ calculated from plots of Eq. (3) from the LED source operated at different irradiance levels (here expressed in mW/cm²).

Irradiance (mW/cm ²)	$\Phi \varepsilon I_0$ (s ⁻¹)
5.0	0.0014
12.8	0.0034
21.6	0.0056

$$\frac{CQ}{CQ_0} = \frac{1}{\varepsilon CQ_0 L} \ln[1 - (1 - e^{\varepsilon CQ_0 L})e^{-\varepsilon \Phi I_0 t}] \quad (4)$$

Fig. 3 shows a typical plot for the volume averaged CQ concentration versus time calculated from transmitted light measurements assuming a decrease in light intensity according to the Beer–Lambert law, i.e., $-\log(I_t/I_0) = \varepsilon CQL$.

The kinetics of photopolymerization of dimethacrylates with the CQ/amine pair was studied by Cook [1] who reported a first-order kinetic expression for CQ loss. The excellent fit (Fig. 3) of the global CQ concentration with the prediction from Eq. (4), demonstrates that, for the CQ/DMAEMA concentration used in this study, the assumption of a first-order kinetic for the decomposition of CQ is satisfactory.

In systems that are well mixed or with very small absorbance, the spatial variation of initiator concentration may be neglected and the concentration of photoinitiator is only function of exposure time. However, under the experimental conditions used in this study, more than 50% of the incident light was absorbed by the CQ at the start of the experiment. At this level of absorbance, the photodecomposition reactions are spatially inhomogeneous and there exists a gradient in the photoinitiator concentration. Initially, the initiator concentration is uniform, and the light intensity will decrease exponentially with depth. Immediately after irradiation, the CQ is consumed at a rate proportional to the local light intensity. This leads to an initiator concentration gradient along the thickness accompanied by a deeper penetration of the light beam. Therefore, the light intensity gradient and the initiator concentration gradient are coupled. The measurements of transmitted light vs. irradiation time provide information about the thickness averaged CQ concentration in the sample. However, a detailed description of the spatiotemporal variation of the local concentration of photoinitiator as well as the photoinitiation rate is obtained from the following expression:

$$-\frac{\partial CQ(z,t)}{\partial t} = \Phi \varepsilon I(z,t) CQ(z,t) \quad (5)$$

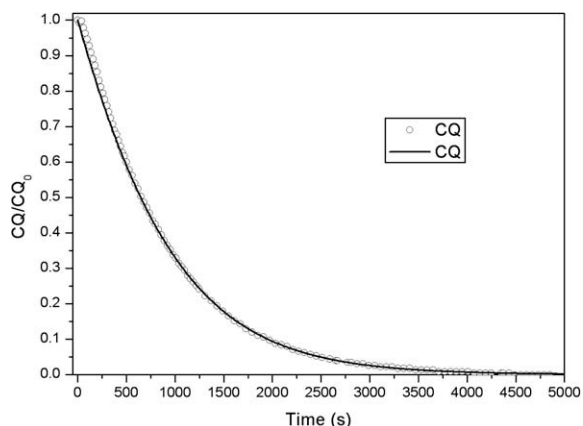


Fig. 3. Normalized global CQ concentration vs. irradiation time calculated from transmission measurements. The sample was 1 mm thick and the irradiance was 5 mW/cm². The solid line corresponds to values calculated from Eq. (5).

where $I(z,t)$ is the irradiance at a depth into the sample – at the irradiated surface $z = 0$, while $z = L$ where the radiation exits the sample. $I(z,t)$ is calculated from the integrated form of the Beer–Lambert law:

$$I(z,t) = I_0 \exp \left[- \int_0^z \varepsilon CQ(z,t) dz \right] \quad (6)$$

The dimensionless local photoinitiator concentration profiles as a function of time and depth into the sample, z , can be calculated from the following analytic solution for the system of Eqs. (5), (6) [8]:

$$\frac{CQ(z,t)}{CQ_0} = [1 - e^{-\varepsilon CQ_0 z/L} (1 - e^{\varepsilon \Phi I_0 t})]^{-1} \quad (7)$$

In the following analysis we assume that the source is monochromatic and that the absorption of the radiation is independent of wavelength. This assumption means that it is assumed that the shape of the spectrum of the radiation on entering and exiting the absorbing medium is the same – a full analysis when this assumption is invalid has recently been published by Kenning et al. [20]. For the 470 nm LED used in the present work, the full width of the spectrum at half height was 28 nm (from 456 to 484 nm) and inside this range the absorbance of CQ varied from 42 (at the 470 nm maximum) to 34 l/mol cm. Calculations of the change in the shapes of the spectra before and after attenuation by CQ shows only small differences and in at the high wavelength end of the spectrum where CQ does not strongly absorb, and so the monochromatic assumption is reasonably valid. However, the radiation from the LED would penetrate further than is calculated here and the effective thickness of the samples are underestimated in the analysis below by approximately 20% and this error has no impact on the conclusions presented here.

The spatiotemporal distributions of photoinitiator concentration and light irradiance were calculated from the photodecomposition rate constant ($\varepsilon \Phi I_0$) for an irradiance equal to 5.0 mW/cm², and the results are presented in Figs. 4 and 5. The relevance of these calculations is that our previous measurements [17] of monomer conversion versus

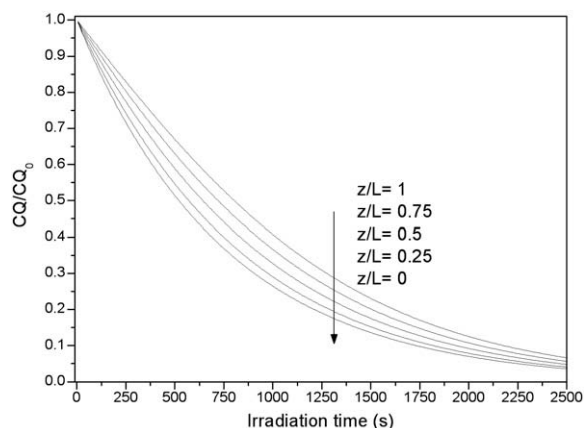


Fig. 4. Dimensionless local photoinitiator concentration vs. irradiation time calculated from Eq. (7) at different depths z . The sample thickness, L , was 1 mm and the irradiance was 5.0 mW/cm².

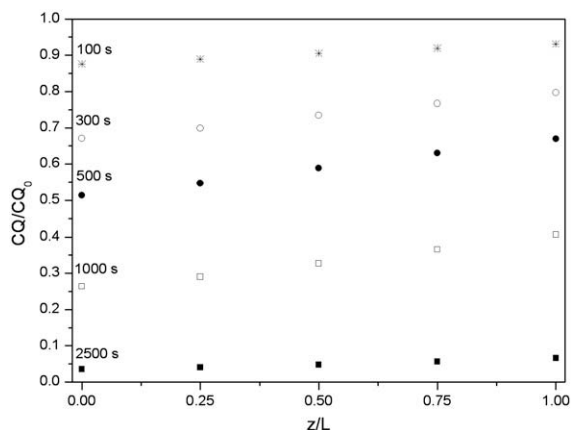


Fig. 5. Dimensionless local photoinitiator concentration profiles along the dimensionless thickness z/L for different irradiation times calculated from Eq. (7) at different depth z into the sample. The sample was $L = 1$ mm thick and the irradiance was 5.0 mW/cm^2 .

irradiation time at that particular irradiance has been undertaken under identical conditions to those used here. Thus, the direct influence of the photobleaching process on the photopolymerization reaction can be examined. The minimum and maximum values of CQ concentration occur at the front and rear surfaces ($z = 0$ and $z = L$) respectively, and the difference between the CQ concentration at $z = 0$ and $z = L$ is a measure of the degree of inhomogeneity in the initiator concentration through sample thickness. The maximum value of the difference is observed when the overall dimensionless CQ concentration is approximately 50%, which occurs at about 650 s irradiation. This is in agreement with results reported by previous research on theoretical treatment of consumption of photobleaching initiators [8]. When absorbance decreases due to photobleaching of the photoinitiator, the radiation attenuation and the non-uniformity of the CQ concentration is reduced as the reaction progresses. As the photoinitiator in the layers nearest to the irradiation source is consumed, light penetrates more readily through the sample thickness which leads to an increase in the rate of photoinitiator consumption in deeper layers. This is illustrated in Fig. 6 which shows the dimensionless local irradiance profiles as a function of the irradiation time and depth.

Light attenuation and photoinitiator photobleaching compete to determine the profiles of initiator concentration and light intensity and consequently, the local photoinitiation rate. The spatio-temporal photoinitiation rate, R_i , was calculated from the photoinitiator consumption rate (Eq. (5)) and the results are presented in Figs. 7 and 8. At short irradiation times and low photoinitiator conversions, the photoinitiation rate in the irradiated surface is markedly higher than that in the rear of the sample. However, during the first 500 s, the photoinitiation rate changes by almost 50% at $z = 0$ (where the radiation enters the sample), whereas the value at $z/L = 1$ (where the radiation exits the sample) changes by <12%. At longer irradiation times and higher levels of photoinitiator decomposition, the opposite trend is observed and the rate of photoirradiation

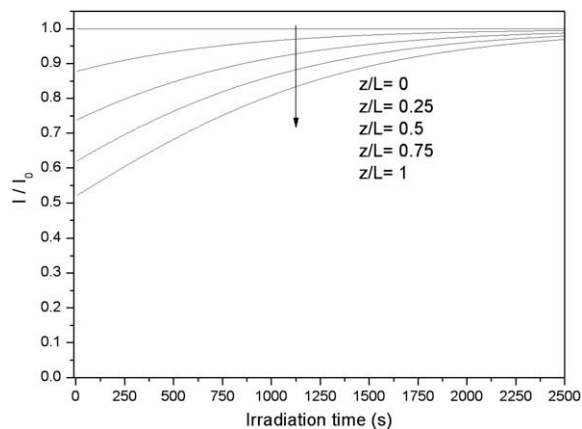


Fig. 6. Dimensionless local irradiance, I/I_0 at various normalized depths (z/L) into the sample as a function of irradiation times, as calculated from Eqs. (6), (7). The sample was 1 mm thick and the irradiance was 5.0 mW/cm^2 .

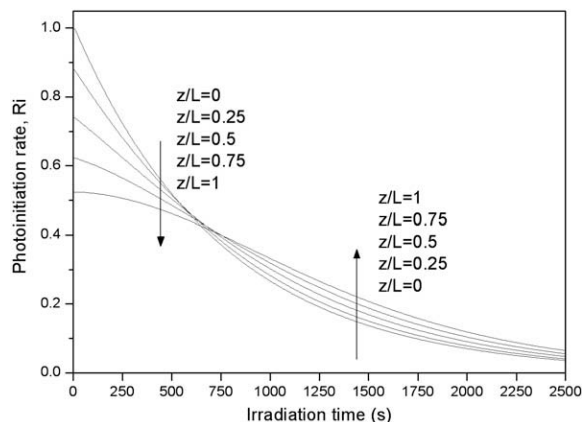


Fig. 7. Dimensionless local photoinitiation rate vs. time calculated from Eq. (6) at different normalized depth z/L . The sample was 1 mm thick and the irradiance was 5.0 mW/cm^2 .

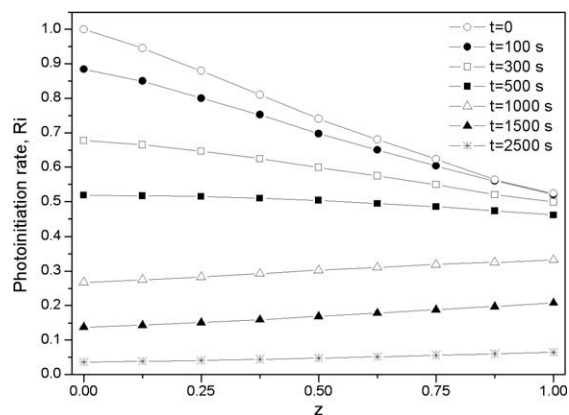


Fig. 8. Dimensionless photoinitiation rate gradients calculated from Eq. (6) at different dimensionless depth z/L . The sample was 1 mm thick and the irradiance was 5.0 mW/cm^2 .

is greatest in layers deeper into the resin because the light intensity for deeper layers is increased due to the photobleaching of the CQ in the upper layers. As a result, the rate of change of photoinitiation rate with depth changes from a negative value to positive when the dimensionless photoinitiation rate is approximately 0.5, according to the profiles presented in Figs. 7 and 8 [8]. The profiles shown in Figs. 4–8 were calculated for the irradiation time required for near-complete photobleaching of the CQ. However, previous measurements of monomer consumption [16] carried out in the same assembly (Scheme 1) and with the same light intensity as that used here demonstrated that the monomer consumption approached a plateau after approximately 320 s irradiation due to vitrification of the crosslinked polymer. Therefore, it is relevant to assess the initiation rate profiles in the time scale required for the polymerization of the resin. The spatio-temporal distributions of photoinitiator concentration, light irradiance and photoinitiation rate during an irradiation period of 320 s for 2 mm thick samples were computed and the results are presented in Figs. 9–11. Fig. 9 shows the influence of sample thickness on the dimensionless CQ concentration as a function of irradiation time and depth. It is seen that the photolysis rate of CQ is relatively slow compared with the polymerization reaction. At the end of the measurements only 22% of the CQ, averaged over the sample thickness, was consumed before the monomer conversion reached a plateau. At a given time and position within the sample, the degree of light attenuation is determined by the absorbance of the layers nearest to the irradiation source. Fig. 10 illustrates the effect of increasing the depth into the sample on the dimensionless local light intensity versus irradiation time. Since the local photoinitiation rate depends on the local light intensity and photoinitiator concentration, when absorbance is increased due to increased sample thickness, the distribution of photoinitiation rate becomes less uniform, as it is illustrated in Fig. 11. The slight increase in the initiation rate at the optical exit in the 2 mm thick sample results from the increase in light irradiance due to upbeam photoinitiator consumption.

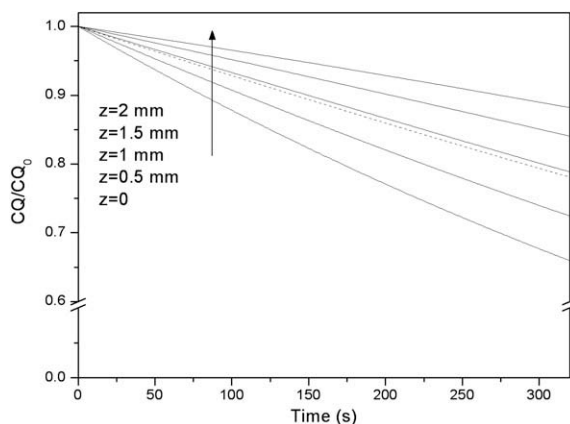


Fig. 9. Changes in dimensionless local photoinitiator concentration during the time required for the resin to vitrify at different depth z . The sample was $L = 2$ mm thick and the irradiance was 5.0 mW/cm^2 . The dotted line corresponds to the volume averaged concentration of CQ.

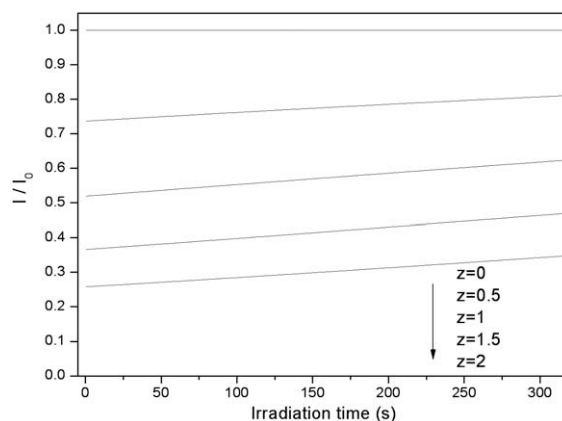


Fig. 10. Changes in dimensionless light irradiance, I/I_0 , at each depth through sample thickness during the time period required for the resin to vitrify. The sample was 2 mm thick and the irradiance was 5.0 mW/cm^2 .

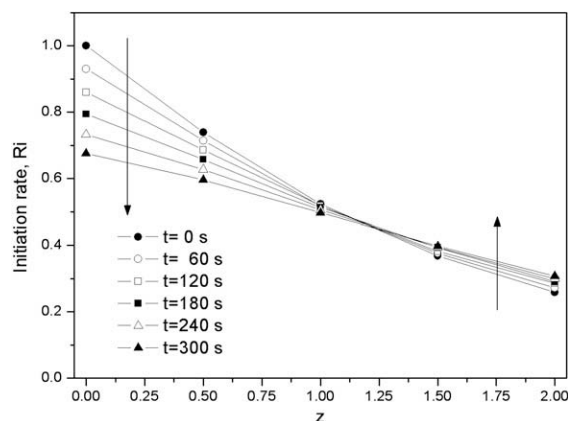


Fig. 11. Dimensionless local photoinitiation rate gradients during the time required for the resin to vitrify. The sample was 2 mm thick and the irradiance was 5.0 mW/cm^2 .

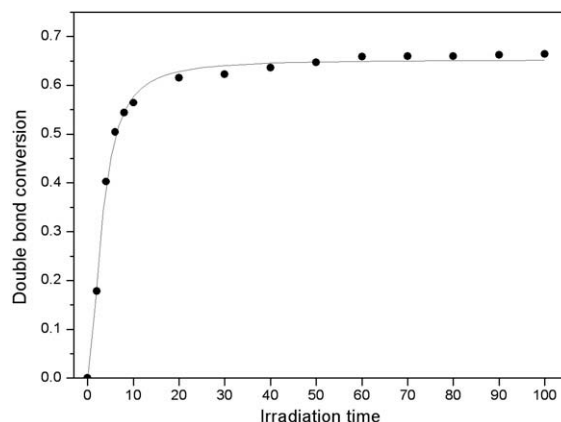


Fig. 12. Global double bond conversion vs. irradiation time for a bis-GMA/TEGDMA 70:30 blend containing 1.5 wt% CQ/DMAEMA. The irradiance of the LED Ultralume was 60 mW/cm^2 . The sample was 3 mm thick. Results from Ref. [4].

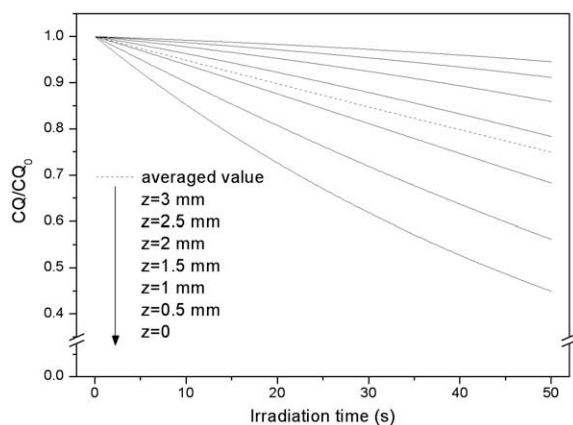


Fig. 13. Changes in dimensionless local photoinitiator concentration during the time required for the resin to vitrify at different depth z . The sample containing 1.5 wt% CQ/DMAEMA was 3 mm thick. The volume averaged concentration of CQ is also plotted. The LED irradiance was 60 mW/cm².

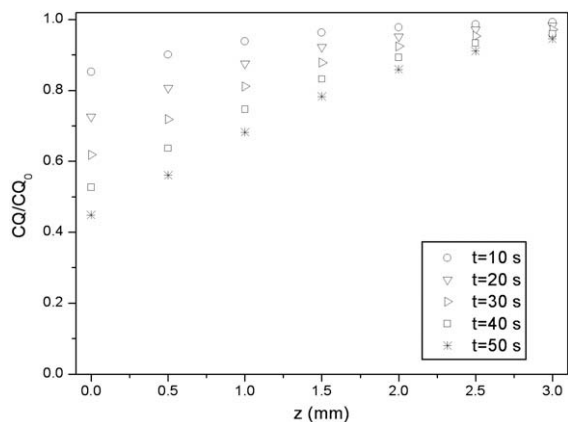


Fig. 14. Changes in dimensionless local photoinitiator concentration gradients during the time required for the resin to vitrify. The sample containing 1.5 wt% CQ/DMAEMA was 3 mm thick. The LED irradiance was 60 mW/cm².

Results presented in Figs. 4–11 were performed for a LED source of relatively low irradiance. These types of LEDs are commonly used in studies of polymerization kinetics because they permit ready monitoring of the progress of extremely rapid polymerization processes. However, for practical purposes it is relevant to analyze the photodecomposition of the CQ when irradiated with light irradiances typical of commercial units. In a previous work [4], the progress of the photopolymerization of a bis-GMA/TEGDMA blend, activated with 1.5 wt% CQ in combination with an equimolar proportion of DMAEMA, was studied during irradiation with a commercial dental LED unit (Ultralume2, Ultradent, USA). This initially high initiator concentration was used in order to achieve polymerization times appropriate for the clinical practice. Layers of 3 mm thickness were irradiated and the global monomer consumption was measured as a function of the irradiation

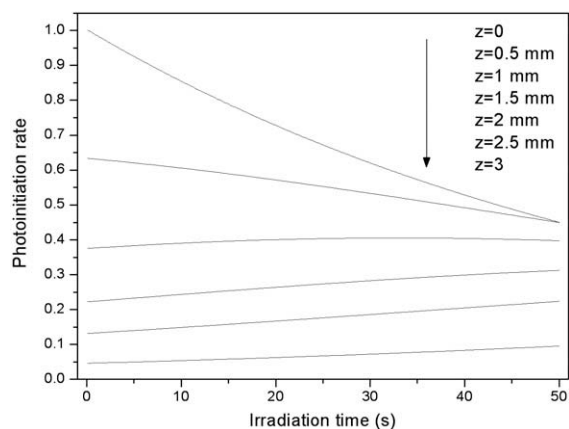


Fig. 15. Dimensionless local photoinitiation rate gradients during the time required for the resin to vitrify. The sample containing 1.5 wt% CQ/DMAEMA was 3 mm thick. The LED irradiance was 60 mW/cm².

time. The irradiance of this commercial LED is 12 times the used in computations presented previously (Table 1). Assuming that the spectral distributions of the OTLH-0090-BU LED and the Ultralume were similar, the photodecomposition rate for the Ultralume source, extrapolated from values presented in Table 1, was 0.015 s⁻¹. As a result of the higher CQ concentration and radiation intensity, Fig. 12 shows that the experimentally determined global double bond conversion reached a plateau after about 50 s irradiation, therefore, computations of the extent of photobleaching were calculated for this time interval.

Figs. 13–15 illustrate the predicted effect of increased irradiance upon the local photoinitiator consumption and initiation rate profiles for the previously reported work [4]. The increased absorbance of this sample due to the higher (1.5 wt%) level of CQ and greater specimen thickness (3 mm) gives a less uniform distribution of photoinitiation rates (Fig. 13) than for the 2 mm thick sample using 1.0 wt% CQ (Fig. 9). As found with the thinner specimen, a comparison of the conversion (Fig. 12) with the photobleaching (Fig. 13) shows that the photobleaching rate is much slower than the polymerization rate. In fact, only 20% of the initial amount of CQ is consumed before the polymerization reaction had almost ceased. It is seen from Figs. 13–15 that the initiation rate decreases rapidly with time near the irradiated surface but it actually increases in the deeper regions of the specimen, as was observed above (see Fig. 7). In addition, during the early stages of the irradiation the photoinitiation rate is much more dependent on the depth into the sample. Thus, the progress of the polymerisation reaction is characterized by a markedly nonuniform distribution of photoinitiation rates and of cure.

4. Conclusions

The global photobleaching kinetics of CQ in thick specimens of the bis-GMA/TEGDMA/ CQ/amine were studied during continuous irradiation. The kinetics were satisfactorily fitted to a kinetic expression based on first order

decomposition kinetics of CQ and the experimentally determined rate constant for CQ loss was proportional to the irradiation intensity in agreement with the photoinitiation mechanism.

The coupled system of equations which describe the photoinitiator decomposition rate and light attenuation according to the Beer-Lambert law was solved so that the gradients of photoinitiator concentration, light intensity and photoinitiation rate along the path of irradiation could be computed. The profiles of initiator concentration and light intensity and, consequently, the local photoinitiation rate are the result of a balance between light attenuation degree and photoinitiator photobleaching rate.

Calculations based on the rate of consumption of CQ in 3 mm thick samples photopolymerized with LED sources of high intensity, revealed that less than 25% CQ was consumed before the polymerization reaction had almost ceased. Thus, the progress of the polymerisation reaction is characterized by a markedly nonuniform photoinitiation rates distribution.

Acknowledgements

The financial support provided by the CONICET, ANPCyT and the ARC (through Grant DP0453104) is gratefully acknowledged. The authors are grateful to Esstech for the generous donation of the Bis-GMA monomer used in this study.

References

- [1] Cook WD. Photopolymerization kinetics of dimethacrylates using the camphorquinone/amine initiator system. *Polymer* 1992;33:600–9.
- [2] Nie J, Linden LA, Rabek JF, Fouassier JO, Morlet-Savary F, Scigalski F. A reappraisal of the photopolymerization kinetics of triethyleneglycol dimethacrylate initiated by camphorquinone-N,N-dimethyl-p-toluidine for dental purposes. *Acta Polym* 1998;49:145–61.
- [3] Schroeder W, Cook WD, Vallo CI. Photopolymerization of N,N-dimethylaminobenzyl alcohol as amine co-initiator for light-cured dental resins. *Den Mater* 2008;24:686–93.
- [4] Shroeder WF, Vallo CI. Effect of different photoinitiator systems on conversion profiles of a model unfilled light-cured resins. *Den Mater* 2007;23:1313–21.
- [5] Senyurt AF, Hoyle CE. Three component ketocoumarin, amine, maleimide photoinitiator II. *Euro Polym J* 2006;42:3133–99.
- [6] Ó'Brien AK, Bowman CN. Modeling thermal and optical effects on photopolymerization systems. *Macromolecules* 2003;36:7777–82.
- [7] Johnson PM, Stansbury JW, Bowman CN. Photopolymer kinetics using light intensity gradients in high-throughput conversion analysis. *Polymer* 2007;48:6319–24.
- [8] Terrones G, Pearlstein AJ. Effects of optical attenuation and consumption of a photobleaching initiator on local initiation rates in potopolymerizations. *Macromolecules* 2001;34:3195–204.
- [9] Terrones G, Pearlstein AJ. Effects of kinetics and optical attenuation on the completeness, uniformity, and dynamics of monomer conversion in free-radical photopolymerizations. *Macromolecules* 2001;34:8894–906.
- [10] Cabral JT, Douglas JF. Propagating waves of network formation induced by light. *Polymer* 2005;46:4230–41.
- [11] Ivanov V, Decker C. Kinetic study of photoinitiated frontal polymerization. *Polym Int* 2001;50:113–8.
- [12] Miller G, Gou I, Narayanan V, Scranton A. Modeling of photobleaching for the photoinitiation of thick polymerization systems. *J Polym Sci Part A: Polym Chem* 2002;40:793–808.
- [13] Désilles N, Gautrelet C, Lecamp L, Lebaudy P, Bunel C. Effect of UV light scattering during photopolymerization on UV spectroscopy measurements. *Euro Polym J* 2005;41:1296–303.
- [14] Azan V, Lecamp L, Lebaudy P, Bunel C. Simulation of the photopolymerization gradient inside a pigmented coating Influence of TiO₂ concentration on the gradient. *Prog Org Coat* 2007;58:70–5.
- [15] Ficka BA, Thiesena AM, Scranton AB. Cationic photopolymerizations of thick polymer systems: Active center lifetime and mobility. *Euro Polym J* 2008;44:98–107.
- [16] Cui Y, Yang J, Zeng Z, Zeng Z, Chen Y. Monitoring frontal photopolymerization by electroresistance. *Euro Polym J* 2007;43:3912–22.
- [17] Mucci V, Arenas G, Duchowicz R, Cook WD, Vallo CI. Influence of thermal expansion on shrinkage during photopolymerization of dental resins based on bis-GMA/TEGDMA. *Dent Mat*, 2009, in press.
- [18] Désilles N, Lecamp L, Lebaudy P, Youssef B, Lebaudy Z, Bunel C. Simulation of conversion profiles within dimethacrylate thick material during photopolymerization. Validation of the simulation by thermal analysis data. Application to the synthesis of a gradient structure material. *Polymer* 2006;47:193–9.
- [19] Chen Y, Ferracane JL, Prahl SA. Quantum yield of conversion of the photoinitiator camphorquinone. *Dent Mater* 2007;23:655–64.
- [20] Kenning N, Kriks D, El-Maazawi M, Scranton A. Spatial and temporal evolution of the photoinitiation rate for thick polymer systems illuminated with polychromatic light. *Polym Int* 2006;55:994–1006.